Effect of *Lantana camara* ethanolic leaf extract on survival and migration of MDA-MB-231 triple negative breast cancer cell line

Arundhaty Pal[#], Sourav Sanyal[#], Sayantani Das, and Tapas Kumar Sengupta*

Department of Biological Sciences

Indian Institute of Science Education and Research Kolkata

Mohanpur, Nadia - 741 246, West Bengal, India

[#]Contributed equally

*Correspondance: senguptk@iiserkol.ac.in

Abstract

Breast cancer is considered as a leading cause of cancer-related death worldwide. The development of chemotherapeutic resistance and the production of undesirable side effects steer the search for new potential candidates with therapeutic implications. *Lantana camara* has been reported to cure a number of ailments, with few studies showing its cytotoxic effect on breast cancer cell lines. However, the impact of *Lantana camara* on triple negative breast cancer cells is largely obscure to date. The present study investigated the effect of ethanolic extract of *Lantana camara* leaves on the triple negative breast cancer cell line, MDA-MB-231. We found that *Lantana camara* leaf extract induced cytomorphological changes and exhibited a growth inhibitory effect on MDA-MB-231 cells in a dose-dependent manner. The extract was observed to induce G0/G1 cell cycle arrest. Nuclear staining of the cells exposed to *Lantana camara* leaf extract suggested the presence of condensed nuclei and the result of flow cytometry analysis confirmed cell death by apoptosis. *Lantana camara* leaf extract also reduced the migration of MDA-MB-231 cells as evidenced by the wound healing assay results. In summary, this study demonstrates the efficacy of the extract to produce growth-inhibitory and anti-migratory effects on MDA-MB-231 cells. Our results thus suggest that *Lantana camara* leaf extract can be considered a potent source of chemotherapeutic agents for triple-negative breast cancer treatment.

Keywords: *Breast Cancer, Lantana camara, MDA-MB-231, apoptosis, migration*

Introduction

Cancer, as a major cause of death and a significant obstacle to increased life expectancy, accounted for approximately 19.3 million new cases and an estimated 10.0 million deaths worldwide in 2020. With 2.3 million new cases (11.7% of all cancer cases), breast cancer is currently the largest cause of cancer incidence and the fifth leading cause of cancer-related deaths worldwide [1].

Breast cancer can be further classified into different molecular subtypes based on immunohistochemical staining: luminal A (ER/PR^+, $HER\text{-}2^-$, $Ki\text{-}67^+ < 20\%$), luminal B ($ER/PR^+ < 20\%$, $HER\text{-}2^-$, $Ki\text{-}67^+ \geq 20\%$); $HER\text{-}2^+$ B2 (ER/PR^+, HER-2 overexpression), HER-2 overexpression (ER^-, PR^-, HER2 overexpression), basal-like Triple Negative Breast Cancer (ER^-, PR^-, $HER2^-$), and other special subtypes [2]. Triple negative breast cancer (TNBC) typically has a higher tumor grade, greater tumor size, higher invasiveness and rate of metastasis, and more frequent recurrence compared to other types of breast cancer [3]. TNBC is most common in premenopausal young women under 40, who make up about 15% to 20% of all breast cancer patients [4]. TNBC patients have a reduced life expectancy, and 40% of them die within the first five years of diagnosis [5].

TNBC is resistant to endocrine therapy and molecular targeted therapy because of its unique molecular profile. Surgical removal, radiation therapy, and chemotherapy are currently used in the treatment of TNBC. Bevacizumab and chemotherapy medications have been utilized in combination to treat TNBC in various countries [6]. But these treatment options have limitations due to lower efficacy, unwanted side effects, and higher cost. Moreover, a considerable number of cancer patients develop resistance to chemotherapy [7]. Tumor reappearance is eventually caused by the remaining metastatic lesions. Therefore, a top priority is to find more effective, safe, and affordable treatments against TNBC.

Natural products, mainly plant-derived phytochemicals play a key role here. Currently, plant-based anti-cancer drugs account for three-quarters of all prescribed medicines. Taxol, vinblastine, vincristine, podophyllotoxin, and camptothecin are some of the most well-known examples [8]. *Curcuma longa*, *Withania somnifera*, *Zingiber officinale*, *Hypericum perforatum*, *Camellia sinensis*, and other medicinal herbs have also shown optimistic anti-breast cancer potential in the research phase [9]. Despite all of these efforts, clinical usage of plant-based chemotherapeutic medicines has been found to fall short of expectations. Thus, there is an ongoing demand for new, effective, and affordable medications that are free of

harmful side effects. A ray of hope is that only 5–15% of the 250,000 higher plants have been screened for therapeutic potential [8]. In this scenario, exploiting the vast richness of unfathomed plants in a tropical country like India is both relevant and reasonable. Bioactive compounds derived from these plants can be treatment options for TNBC.

Lantana camara, also known as red or wild sage, is an invasive weed of the Verbenaceae family. More than 60 different countries of tropical, subtropical, and temperate regions are home to this flowering species [10]. All the parts of *L. camara*, especially leaves have been utilized in herbal medicines for generations to treat various illnesses such as headache, fever, skin itches, ulcers, rheumatism, measles, chicken pox, asthma, and leprosy [11, 12]. *L. camara* leaves also show anti-bacterial, anti-fungal, nematocidal, insecticidal, and anti-oxidant properties [13]. Various studies have also reported that different extracts of *L. camara* leaves display anti-cancer activity. Human lung carcinoma cell line (A549) and mouse melanoma (B16F10) revealed *in vitro* cytotoxicity when exposed to *L. camara* leaf methanolic extract [14]. Another study has reported that ethanolic extract of *L. camara* inhibited proliferation and induced apoptosis of MCF-7 breast cancer cell line [15].

However, the effects of *L. camara* leaf ethanolic extract (LCLE) against triple-negative breast cancer cells has not yet been identified. It is also noteworthy that the level and kind of phytochemicals present in various *Lantana* species are reported to be quite varied [16]. Therefore, in this present study, we investigated the effects of *L. camara* (from Mohanpur, Nadia, West Bengal, India) leaf ethanolic extract on cell death and migration in the TNBC cell line MDA-MB-231.

Materials and methods

Cell culture

MDA-MB-231 cell line was obtained from National Centre for Cell Science (NCCS), Pune, India, and maintained in Dulbecco's Modified Eagle Medium (DMEM) High Glucose (HiMedia, India) supplemented with 10% (v/v) Fetal Bovine Serum (FBS) (HiMedia, India), 10000 U/ml Penicillin and 10 mg/ml Streptomycin antibiotic solution (HiMedia, India). Cells were incubated at 37ºC in 95% air in a humidified incubator with 5% CO_2. 1X Trypsin-EDTA solution (HiMedia, India) was used for cell harvesting during sub-culturing.

Lantana camara leaf extract (LCLE) preparation

Healthy leaves of *Lantana camara* were collected from the campus and surroundings of the Indian Institute of Science Education and Research Kolkata (lattitude-22°57′50′′N and longitude-88°31′28′′E). The collected plant leaves were rinsed with tap water, followed by distilled water then shade-dried at 30°C for 48 hours. Dried leaves were ground into a fine powder using mortar and pestle and then subjected to extraction with absolute ethanol in a ratio of 1:10 (w/v) by gentle mixing on an orbital shaker at 37°C for 18 hours. The extracted mixture was filtered using Whatman No. 2 filter paper and the filtrate was concentrated using a rotary evaporator under low pressure and 37°C temperature. The resultant extract residues were then collected and dissolved in molecular-grade ethanol (Merck, Germany) to prepare stock solution as required. This stock solution was filtered using a syringe filter (0.22 micron) and was kept in 4°C for future use. 0.8% (v/v) ethanol was used as vehicle control in each experiment and the final ethanol percentage did not exceed 0.8% (v/v) in any of the experimental conditions.

Cell morphology analysis

MDA-MB-231 cells were seeded in 35mm dishes (0.15 $x10^6$ cells/dish) and incubated overnight. The spent medium was then discarded and cells were treated with different doses of LCLE for 24 hours. Cell morphology was examined and images were captured using an inverted microscope (IX81, Olympus, Japan) with a camera (photomterics, CoolSNAP MYO) under 40X magnification.

Cell viability assay

The cytotoxicity of LCLE was tested on MDA-MB-231 cells by 3-(4,5-dimethylthiazol-2-yl)-2,5-diphenyltetrazolium bromide (MTT) colorimetric assay. Cells were seeded in a 96-well plate ($0.5x10^4$ cells/well) and incubated overnight. Cells were then treated with different doses of LCLE for 24 hours. After treatment, spent media from the wells was discarded, fresh complete media with a final concentration of 0.5 mg/ml of MTT solution (SRL, India) was added to each well and the cells were incubated in dark at 37°C and 5% CO_2 for 4 hours. Thereafter, the MTT containing medium was carefully aspirated from the plate, 100 µl of dimethyl sulfoxide (DMSO) was added to each well and incubated for 30 minutes in dark at 37°C. Then absorbance was measured in microplate reader (Biotek, Agilent technologies, CA, USA) using Gene5 software at 595 nm. The cytotoxic effect of the leaf extract was expressed as viability percentage in comparison to vehicle control. Dose response curve was created by using GraphPad Prism 6.01 (GraphPad software, CA, USA).

Cell cycle phase distribution assay

MDA-MB-231 cells were seeded in 35 mm cell culture dishes (0.15 x10^6 cells/dish) and incubated overnight. Cells were then treated with different doses of LCLE along with vehicle. Following 24 hours of treatment, cells were harvested from the culture dishes by treating with 1X Trypsin-EDTA and collected along with the floating cells derived from spent media. Cell pellets were washed with ice-cold 1X phosphate buffered saline (PBS). Then the cells were fixed with 70% ethanol and incubated at 4°C overnight. This was followed by washing the cells with ice-cold 1X PBS and resuspension in 500 µl propidium iodide (PI) solution [475 µl 1X PBS+20 µl PI (HiMedia, India) from 1 mg/ml stock+5 µl RNase A (HiMedia, India) from 20 mg/ml stock)] and incubated at 37°C for 20 minutes in dark. Thereafter, the PI solution was removed and cells were resuspended using 500 µl 1X PBS and the samples were analyzed by using BD FACS Fortessa flow cytometer (BD Biosciences, USA). Cell cycle distribution was (Sub-G1, G1/G0, S and G2/M) determined and graph was plotted by using GraphPad Prism 6.01 (GraphPad software, CA, USA).

Nuclear morphological analysis by DAPI staining

MDA-MB-231 cells (0.15 x10^6 cells/well) were seeded in a 24-well plate containing coverslips and then treated with different doses of LCLE and vehicle for 24 hours. Following treatment, media was removed and the wells (with coverslips) were washed with 1X D-PBS (1X PBS with 0.9 mM calcium chloride dehydrate and 0.5 mM magnesium chloride hexahydrate). Cells were further fixed by adding ice-cold 4% paraformaldehyde and incubated for 15 minutes at room temperature. After fixation, cells on the coverslips were washed with 1X PBS and then permeabilized by adding permeabilization buffer [1X D-PBS + 0.5% Tween 20] and incubated for 20 mins. Then the cells were washed with 1X PBS, 1 µg/ml of 4',6-diamidino-2-phenylindole (DAPI) solution (in 1X PBS) was added to each well (with coverslip) and incubated for 15 minutes in dark. Cells were again washed with 1X PBS; coverslips were removed from the wells, mounted on clean glass slides using 5% glycerol as mounting agent and sealed. The slides were observed and images were captured under inverted microscope (IX81, Olympus, Japan) with a camera (photomterics, CoolSNAP MYO).

Annexin V-FITC/PI double staining

Apoptotic and non-apoptotic cells were differentiated using the Annexin V-FITC Apoptosis detection kit (BD biosciences, USA) according to the manufacturer's protocol. MDA-MB-231 cells (0.2 x10^6cells/dish) were seeded in 35 mm culture dish and then treated with different

doses of LCLE and vehicle for 24 hours. Following treatment, cells were harvested from the culture dishes by treating with 1X Trypsin-EDTA and collected along with the floating cells derived from spent media. Cell pellet was once washed with ice-cold 1X PBS and then resuspended in 100 µl of 1X binding buffer. 5 µl each of Annexin V-FITC and Propidium iodide was added for staining and gently vortexed followed by incubation in dark for 15 minutes at room temperature. Finally, 400 µl of 1X binding buffer was added to each tube and the samples were analyzed within an hour by using BD FACS Fortessa flow cytometer (BD Biosciences, USA). The percentage of apoptotic and non-apoptotic cell population was determined by evaluating the relative amount of Annexin V-FITC positive alone cells (early apoptosis), both Annexin V-FITC and PI-positive cells (late apoptosis) and PI positive alone cells (non-apoptotic). Cell population negative for both Annexin V-FITC and PI was considered to be of viable cells. Data was represented graphically by using GraphPad Prism 6.01 (GraphPad software, CA, USA).

Wound healing assay

MDA-MB-231 cells (0.2 x10^6 cells/dish) were seeded in 35 mm dish and grown until a uniform monolayer of cells was formed. Once a monolayer was formed, a wound was created in each dish using a sterile P10 microtip and the spent media was removed from the culture dish. The monolayer of cells was washed twice with 1XPBS, complete media was added to the cells followed by addition of cycloheximide (0.5 µg/ml). Immediately after addition of cycloheximide, the wounded cells were treated with different doses of LCLE and vehicle. The cells were imaged at 0 h post treatment using inverted microscope (IX81, Olympus, Japan) with a camera (photomterics, CoolSNAP MYO). The cells were incubated at 37ºC in 95% air in a humidified incubator with 5% CO_2 and images were intermittently captured at 12 h and 24 h post treatment. The images were analyzed and wound closure was calculated by ImageJ 1.54b (ImageJ software, NIH, USA) using the following formula:

$$\text{Wound closure \%} = \frac{\text{Area of wound at time 0 h - Area of wound at time 't' h}}{\text{Area of wound at time 0 h}} \text{ X 100 \%}$$

where t = specific time intervals after 0 h

Data was represented graphically by using GraphPad Prism 6.01 (GraphPad software, CA, USA).

Statistical analysis

All experiments were conducted for atleast three times and data was represented as mean ± SEM. Data was plotted using Graphpad Prism 6.01 (GraphPad software, CA, USA) and statistical analysis was done by performing parametric Student's t-test. $P<0.05$ was considered to indicate a statistically significant difference.

Results

LCLE produced cytotoxic effects in MDA-MB-231 cells

MDA-MB-231 cells have spindle-shaped morphology under normal culture condition. To evaluate whether LCLE induced any morphological changes, MDA-MB-231 cells were exposed to 40 µg/ml, 80 µg/ml, 120 µg/ml and 150 µg/ml of leaf extract, and vehicle (0.8% ethanol) for 24 hours and the morphology of the cells were observed. Images were captured at 0 h and 24 h after treatment with LCLE using a phase-contrast microscope under 40X magnification. Figure 1A exhibited that lower doses of LCLE (40 µg/ml and 80 µg/ml) treated-MDA-MB-231 cells were shorter in length and cell shrinkage was observed at 80 µg/ml dose of extract. Further, it was observed that at 120 µg/ml and 150 µg/ml of LCLE treatments caused the MDA-MB-231 cells to appear more spherical abandoning the typical spindle-shaped morphology when compared to the vehicle-treated or untreated control cells. The spherical cells ceased to tether to the surface of the treatment dishes and were freely suspended in the medium. Thus it was found that LCLE was able to induce morphological changes in MDA-MB-231 cells as compared to vehicle-treated or untreated control cells.

The induction of morphological changes was indicative of a certain cytotoxic effect being imposed by the extract. To understand whether altered morphology is due to the induction of cytotoxicity by leaf extract, MDA-MB-231 cells were treated with various doses of the leaf extract for 24 hours and the viability of LCLE-treated MDA-MB-231 cells was evaluated using MTT assay. The graph in Figure 1B represents dose-dependent viability of MDA-MB-231 cells where the viability of vehicle-treated cells was considered to be 100%. It was observed that leaf extract impeded the viability of the cells in a dose-dependent manner. Half-maximal inhibitory concentration (IC_{50}) of the extract was found to be 111.33 µg/ml. These results combined, indicated that *L.camara* leaf extract has an inhibitory effect on the viability of MDA-MB-231 cells.

Induction of G0/G1 cell cycle arrest by LCLE in MDA-MB-231 cells

To further evaluate the mechanism of the anti-proliferative effect of LCLE, we analysed cell-cycle phase distribution using flow cytometry. Our data (Figure 2A) showed a representative image of the distribution of MDA-MB-231 cells in the different phases of cell cycle (Sub-G1, G0/G1, S and G2/M) when treated for 24 hours with 60 μg/ml, 80 μg/ml, 100 μg/ml and 120 μg/ml of LCLE along with vehicle treated and untreated control. Analyzing our data (Figure 2B) revealed that G0/G1 population increased to 78.80% ± 1.58 % , 79.68% ± 2.07%, 78.15% ± 2.17 % and 75.98% ± 3% in 60 μg/ml, 80 μg/ml, 100 μg/ml and 120 μg/ml leaf extract treated cells respectively whereas vehicle treated cells had 61.35% ± 2.6 % of G0/G1 population. This finding implied that treatment with LCLE induced arrest at G0/G1 phase, which remained essentially unaltered even with increase in dose. Increase in G0/G1 population was also accompanied by decrease in S-phase population to 4.73% ± 0.48% in 120 μg/ml of leaf extract treated cells as compared to the 15.21% ± 13.9% of cell population in vehicle treated cells. Similar trend of decline in G2/M population was also observed in LCLE treated cells, where the cells treated with 120 μg/ml of the extract had 12.01% ± 1.87% population but the vehicle control had 20.95%± 2.00% of cells in G2/M phase. In the sub-G1 population slight increase in percentage of cell population was also observed. The sub-G1 population increased from 2.47% ± 0.59% in vehicle treated cells to 7.26% ± 2.68% in 120 μg/ml of extract treated MDA-MB-231 cells. Taken together, our result established that LCLE induced dose-independent G0/G1 arrest in MDA-MB-231 cells accompanied by reduction in S and G2/M population as compared to vehicle control cells.

Nuclear condensation was induced by LCLE

To further understand the underlying mechanism of cytotoxicity imposed by LCLE, we analyzed chromatin condensation and nuclear fragmentation of MDA-MB-231 cells by staining using the DNA-binding fluorescent dye, DAPI (4',6-diamidino-2-phenylindole). Cells were treated with 60 μg/ml, 120 μg/ml and 150 μg/ml of LCLE. In Figure 3, it was observed that with increase in the dose of the leaf extract, nuclear condensation and fragmentation was induced in the cells. The corresponding DIC images also corroborated the overall morphological changes induced (as observed earlier in Figure 1A) by LCLE treatment. In contrast, untreated and vehicle treated cells displayed uniform chromatin staining and unaltered cellular morphology.

LCLE promoted apoptosis in MDA-MB-231 cells

The induction of nuclear condensation and fragmentation by LCLE was partially indicative of programmed cell death. To elucidate whether the growth inhibitory effects of the extract was due to apoptosis-mediated cell death, MDA-MB-231 cells were exposed to 60 μg/ml, 120 μg/ml and 180 μg/ml of LCLE for 24 hours. Vehicle and extract treated cells were analysed by flow cytometry after double staining with Annexin V-FITC/ PI. Figure 4A represents scatter plot displaying the distribution of cells after Annexin V-FITC/ PI double staining, where lower left quadrant represents viable cells, lower right quadrant represents early apoptotic population, late apoptotic population is reflected in upper right and non-apoptotic population is represented in upper left quadrant. Graphical representation in Figure 4B showed that LCLE induced apoptotic cell death in a dose-dependent manner. Compared to vehicle control, 60 μg/ml of extract-treated cells had very slight increase in early apoptotic population, late apoptotic and non-apoptotic population. There was a sharp increase in early, late and non- apoptotic population when the cells were exposed to near IC_{50} dose, i.e., 120 μg/ml. However, the maximum decrease in cellular viability was observed when the cells were treated with 180 μg/ml dose of the extract. The percentage of viable cells decreased from (92.14 ± 0.94) % in vehicle-treated cells to (64.67 ± 1.97) % in 180 μg/ml extract treated cells. There was a steep increase in early and late apoptotic population when the cells were treated with 180 μg/ml of LCLE. The above findings culminated in the fact that LCLE induced death in MDA-MB-231 cells mainly by the process of apoptosis.

Migration of MDA-MB-231 cells was impeded by LCLE

The ability of cancer cells to migrate is indispensable for initiation of metastasis. An efficient therapeutic approach includes restriction of migration potential of the cancer cells. To assess the impact of LCLE on migration potential of MDA-MB-231, cells were treated with below IC_{50} doses of the extract and wound was given in presence of 0.5 μg/ml of Cycloheximide. As shown in Figure 5A, in comparison to vehicle control, lesser wound area was healed by the cells treated with LCLE. The graphical representation of the wound closure percentage (Figure 5B) indicated that although at 12 h after treatment the wound closure activity was not suppressed significantly, but at 24 h significant impediment to wound closure activity was observed in the presence of LCLE. It was seen that the migratory potential of MDA-MB-231 cells was drastically reduced in a dose-independent manner, where the wound closure % was 60.27 ± 5.12 for vehicle control, it was found to be 42.08 ± 1.68, 40.05 ± 3.11 and 38.04 ±

10.38 for 40 μg/ml, 60 μg/ml and 80 μg/ml LCLE respectively. Thus, our result clearly demonstrated that LCLE impeded the migration ability of MDA-MB-231 cells.

Discussion

Treatment of triple negative breast cancer is challenging as it is generally impervious to the conventional hormone therapy [17]. On the other hand, efficacy of chemotherapy is often plagued by undesirable side effects, some of which often lead to fatal consequences. Around the globe, *Lantana camara* is extensively used to treat several disorders such as fever, asthma, chicken pox, rheumatism, ulcers and many others [18, 19]. The bioactive constituents of *L. camara* like triterpenoids have been reported to exert cytotoxic effects on various cancers including breast cancer [20, 21]. However, the knowledge about how *L. camara* affects MDA-MB-231 cells (a triple negative breast cancer cell line) is largely obscure.

Here in this study, we have observed that LCLE produced morphological changes in MDA-MB-231 cells (Fig. 1A). The noticeable alteration in the morphologies of the cells in the presence of the extract was indicative of cytotoxic stimulation. The experimental results from cell viability assays ascertained that the cytotoxic effect was mediated by a decline in the viability of the cells (Fig. 1B). From the MTT assay result, the IC_{50} value of the leaf extract was determined which was found to be ~111.33 μg/ml. The balance between cellular proliferation and progression through cell cycle is intricately maintained. The inhibitory effect of the extract on the proliferation of MDA-MB-231 cells was found to be correlated with the induction of cell cycle arrest (Fig 2A and 2B) at G0/G1 stage. The accumulation of cells in G0/G1 phase was found to be nearly constant irrespective of the dose of the extract. Regulation of cell cycle and cell death have overlapping effectors, hence induction of prolonged cell cycle arrest often leads to cell death in some cases. Our study showed that the sub-G1 population was increasing slightly upon treatment with LCLE. An increase in the sub-G1 population is suggestive of nuclear fragmentation and hence visualization of nuclear morphology was essential under these circumstances. Staining the extract treated MDA-MB-231 cells with DAPI exhibited increase in nuclear condensation at sub-IC_{50} dose (60 μg/ml) whereas fragmentation was observed at higher doses such as 120 μg/ml and 150 μg/ml (Fig. 3). Several studies have reported that chromatin condensation is a signature of various forms of cell death including apoptosis and non-apoptotic cell death mechanisms such as NETosis, pyroptosis and parthanatos [22]. Among these, DNA fragmentation is characteristic feature in immune

reactive and mitochondria-dependent programmed cell death modalities namely pyroptosis and parthanatos respectively [23, 24]. The cumulative interpretation from our data exhibiting growth-inhibitory, cell cycle arrest inducing and chromatin fragmentation effect directed us to further delineate the mode of cell death. LCLE treated MDA-MB-231 cells were double stained using Annexin V-FITC and PI and it was observed that at near and above IC_{50} doses (120 μg/ml and 180 μg/ml) the plant extract induced apoptotic as well as non-apoptotic cell death (Fig. 4A and 4B). However, at sub-IC_{50} dose (60 μg/ml) there was no noticeable increase in apoptotic or non-apoptotic population when compared to the vehicle-treated cells. In conclusion, the growth inhibitory effect of LCLE could be largely attributed to its ability to induce cell cycle arrest and at the same time its potential to initiate apoptosis.

The ability of cancer cells to migrate is crucial for tumor metastasis [25]. Potential therapeutic strategies are directed towards restricting the motility of cancer cells. MDA-MB-231 cells being an aggressive metastatic TNBC cell line have an inherent capability to migrate [26]. Hence, the efficacy of the extract on the migratory capacity of the cells was evaluated in this study. For this experimental purpose, cells were mainly exposed to the sub-IC_{50} doses so as to invalidate any prominent cytotoxic effect being induced by LCLE, which in turn might alter the wound area. We could establish through our results that LCLE decreased the wound healing capacity of the cells, mainly after 24 hours of treatment irrespective of the doses used. Our finding hence established that LCLE suppressed the migratory potential of MDA-MB-231 cells.

Various chemotherapeutic drugs like Paclitaxel, Vincristine, and Sulforaphane, which have their origin in plants, have been proven effective against cancer [27]. The present study has elucidated that *Lantana camara* is capable of combating the aggressive nature of MDA-MB-231 cells by exhibiting a dual role in triggering cellular death and hindering the motility of the cells as well. The antiproliferative effect of natural plant products is mainly attributed to the presence of bioactive compounds in them. Hence, further isolation and identification of the bioactive compounds in LCLE and studying their implications on triple negative cancer cells would provide a future platform in breast cancer therapy.

Acknowledgements

All authors would like to acknowledge Prof. Subhajit Bandyopadhyay for providing rotary-evaporator facility. The authors would also like to acknowledge Mr. Ritabrata Ghosh and Mr. Tamal Ghosh for their technical support in epifluorescence microscopy and flow-cytometry respectively. AP and SS acknowledge the Department of Biotechnology, Government of India (DBT-India) for research fellowship. SD acknowledges IISER Kolkata for the Postdoctoral Fellowship.

Author Contributions

AP, SS, SD and TKS conceived the study and designed the experiments.

AP, SS and SD did the experiments. AP, SS, SD and TKS analyzed the data and wrote the manuscript.

Funding

The study was funded by IISER Kolkata.

Availability of Data and Materials

In this study, all data generated or analyzed are included in the article.

Declarations

Conflict of interest

The authors declare that there is no conflict of interest.

Ethical Approval

Not applicable.

Consent to Participate

All authors had consented to participate in the study.

Consent for Publication

All authors have given consent for publication.

References

1. Sung, H., Ferlay, J., Siegel, R. L., Laversanne, M., Soerjomataram, I., Jemal, A., & Bray, F. (2021). Global cancer statistics 2020: Globocan estimates of incidence and mortality worldwide for 36 cancers in 185 countries. CA: A Cancer Journal for Clinicians, 71(3), 209–249. https://doi.org/10.3322/caac.21660
2. Goldhirsch, A., Winer, E. P., Coates, A. S., Gelber, R. D., Piccart-Gebhart, M., Thürlimann, B., Senn, H.-J., Albain, K. S., André, F., Bergh, J., Bonnefoi, H., Bretel-Morales, D., Burstein, H., Cardoso, F., Castiglione-Gertsch, M., Coates, A. S., Colleoni, M., Costa, A., Curigliano, G., … Wood, W. C. (2013). Personalizing the treatment of women with early breast cancer: Highlights of the st gallen international expert consensus on the primary therapy of early breast cancer 2013. Annals of Oncology, 24(9), 2206–2223. https://doi.org/10.1093/annonc/mdt303
3. Liang, F., Zhang, H., Gao, H., Cheng, D., Zhang, N., Du, J., Yue, J., Du, P., Zhao, B., & Yin, L. (2020). Liquiritigenin decreases tumorigenesis by inhibiting DNMT activity and increasing BRCA1 transcriptional activity in triple-negative breast cancer. Experimental Biology and Medicine, 246(4), 459–466. https://doi.org/10.1177/1535370220957255
4. Morris, G. J., Naidu, S., Topham, A. K., Guiles, F., Xu, Y., McCue, P., Schwartz, G. F., Park, P. K., Rosenberg, A. L., Brill, K., & Mitchell, E. P. (2007). Differences in breast carcinoma characteristics in newly diagnosed African–american and Caucasian patients. Cancer, 110(4), 876–884. https://doi.org/10.1002/cncr.22836
5. Dent, R., Trudeau, M., Pritchard, K. I., Hanna, W. M., Kahn, H. K., Sawka, C. A., Lickley, L. A., Rawlinson, E., Sun, P., & Narod, S. A. (2007). Triple-negative breast cancer: Clinical features and patterns of recurrence. Clinical Cancer Research, 13(15), 4429–4434. https://doi.org/10.1158/1078-0432.ccr-06-3045
6. Yin, L., Duan, J.-J., Bian, X.-W., & Yu, S.-cang. (2020). Triple-negative breast cancer molecular subtyping and treatment progress. Breast Cancer Research, 22(1). https://doi.org/10.1186/s13058-020-01296-5
7. Housman, G., Byler, S., Heerboth, S., Lapinska, K., Longacre, M., Snyder, N., & Sarkar, S. (2014). Drug resistance in cancer: An overview. Cancers, 6(3), 1769–1792. https://doi.org/10.3390/cancers6031769

8. Soumya, T., Lakshmipriya, T., Klika, K. D., Jayasree, P. R., & Manish Kumar, P. R. (2021). Anticancer potential of rhizome extract and a labdane diterpenoid from Curcuma mutabilis plant endemic to Western Ghats of India. Scientific Reports, 11(1). https://doi.org/10.1038/s41598-020-79414-8
9. Gospodinova, Z. I., Zupkó, I., Bózsity, N., Manova, V. I., Georgieva, M. S., Todinova, S. J., Taneva, S. G., Ocsovszki, I., & Krasteva, M. E. (2020). cotinus coggygria scop. induces cell cycle arrest, apoptosis, genotoxic effects, thermodynamic and epigenetic events in MCF7 breast cancer cells. Zeitschrift Für Naturforschung C, 76(3-4), 129–140. https://doi.org/10.1515/znc-2020-0087
10. Ghisalberti, E. L. (2000). Lantana Camara L. (Verbenaceae). Fitoterapia, 71(5), 467–486. https://doi.org/10.1016/s0367-326x(00)00202-1
11. Hernández, T., Canales, M., Avila, J. G., Duran, A., Caballero, J., Vivar, A. R. de, & Lira, R. (2003). Ethnobotany and antibacterial activity of some plants used in traditional medicine of Zapotitlán de las Salinas, Puebla (México). Journal of Ethnopharmacology, 88(2-3), 181–188. https://doi.org/10.1016/s0378-8741(03)00213-7
12. Mahdi-Pour, B., Jothy, S. L., Latha, L. Y., Chen, Y., & Sasidharan, S. (2012). Antioxidant activity of methanol extracts of different parts of Lantana Camara. Asian Pacific Journal of Tropical Biomedicine, 2(12), 960–965. https://doi.org/10.1016/s2221-1691(13)60007-6
13. Kumar, M. S., & Maneemegalai, S. (2008). Evaluation of larvicidal effect of Lantana camara Linn against mosquito species Aedes aegypti and Culex quinquefasciatus. Advances in Biological Research, 2(3-4), 39-43.
14. Raghu, C., Ashok, G., Dhanaraj, S. A., Suresh, B., & Vijayan, P. (2004). In vitro cytotoxic activity of Lantana camara Linn. Indian journal of pharmacology, 36(2), 94.
15. Han, E. B., Chang, B. Y., Jung, Y. S., & Kim, S. Y. (2014). Lantana Camara induces apoptosis by bcl-2 family and Caspases Activation. Pathology & Oncology Research, 21(2), 325–331. https://doi.org/10.1007/s12253-014-9824-4
16. Sharma, O. P., Vaid, J., & Sharma, P. D. (1991). Comparison of LANTADENES content and toxicity of different taxa of the Lantana plant. Journal of Chemical Ecology, 17(11), 2283–2291. https://doi.org/10.1007/bf00988008
17. Neophytou, C., Boutsikos, P., & Papageorgis, P. (2018). Molecular mechanisms and emerging therapeutic targets of triple-negative breast cancer metastasis. Frontiers in Oncology, 8. https://doi.org/10.3389/fonc.2018.00031

18. Taoubi, K., Fauvel, M., Gleye, J., Moulis, C., & Fourasté, I. (1997). Phenylpropanoid glycosides fromlantana camaraandlippia multiflora. Planta Medica, 63(02), 192–193. https://doi.org/10.1055/s-2006-957647
19. Chhabra, S. C., Mahunnah, R. L. A., & Mshiu, E. N. (1993). Plants used in traditional medicine in eastern Tanzania. vi. angiosperms (sapotaceae to Zingiberaceae). Journal of Ethnopharmacology, 39(2), 83–103. https://doi.org/10.1016/0378-8741(93)90024-y
20. Shamsee, Z. R., Al-Saffar, A. Z., Al-Shanon, A. F., & Al-Obaidi, J. R. (2018). Cytotoxic and cell cycle arrest induction of pentacyclic triterpenoides separated from Lantana Camara leaves against MCF-7 cell line in vitro. Molecular Biology Reports, 46(1), 381–390. https://doi.org/10.1007/s11033-018-4482-3
21. Inada, A., Nakanishi, T., Tokuda, H., Nishino, H., & Sharma, O. (1997). Anti-tumor promoting activities of lantadenes on mouse skin tumors and mouse hepatic tumors. Planta Medica, 63(03), 272–274. https://doi.org/10.1055/s-2006-957673
22. Yan, G., Elbadawi, M., & Efferth, T. (2020). Multiple cell death modalities and their key features (review). World Academy of Sciences Journal. https://doi.org/10.3892/wasj.2020.40
23. Lacey, C. A., Mitchell, W. J., Dadelahi, A. S., & Skyberg, J. A. (2018). Caspase-1 and caspase-11 mediate pyroptosis, inflammation, and control of Brucella joint infection. Infection and Immunity, 86(9). https://doi.org/10.1128/iai.00361-18
24. Fatokun, A. A., Dawson, V. L., & Dawson, T. M. (2014). Parthanatos: Mitochondrial-linked mechanisms and therapeutic opportunities. British Journal of Pharmacology, 171(8), 2000–2016. https://doi.org/10.1111/bph.12416
25. Mehlen, P., & Puisieux, A. (2006). Metastasis: A question of life or death. Nature Reviews Cancer, 6(6), 449–458. https://doi.org/10.1038/nrc1886
26. Huang, Z., Yu, P., & Tang, J. (2020). characterization of triple-negative breast cancer MDA-MB-231 cell spheroid model. OncoTargets and Therapy, Volume 13, 5395–5405. https://doi.org/10.2147/ott.s249756
27. Greenwell, M., & Rahman, P. K. (2015). Medicinal Plants: Their Use in Anticancer Treatment. International journal of pharmaceutical sciences and research, 6(10), 4103–4112. https://doi.org/10.13040/IJPSR.0975-8232.6(10).4103-12

Figure 1

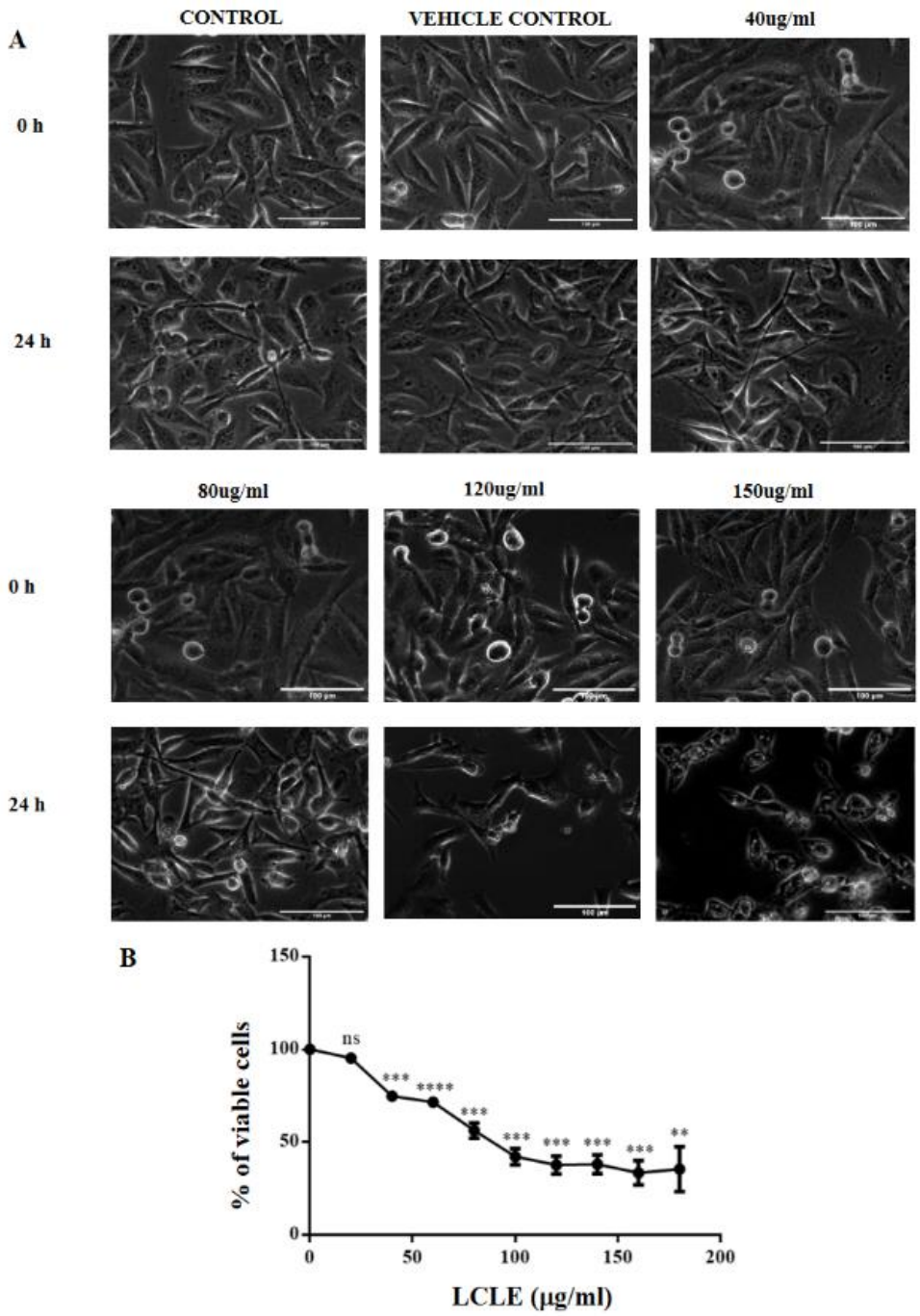

Figure 1. LCLE produced cytotoxic effects in MDA-MB-231 cells. (A) MDA-MB-231 cells treated with different concentrations of LCLE for 24 hours, and images were captured at 0 hours and 24 hours after treatment. **(B)** MDA-MB-231 cells were treated with different concentrations of LCLE for 24 hours, and the viability of the cells were evaluated by MTT assay. Scatter plot distribution is represented as means ± SEM of three independent biological replicates where * is P≤0.05, ** (P≤0.01), *** (P≤0.001) and **** (P≤0.0001) and ns signifies non-significant.

Figure 2

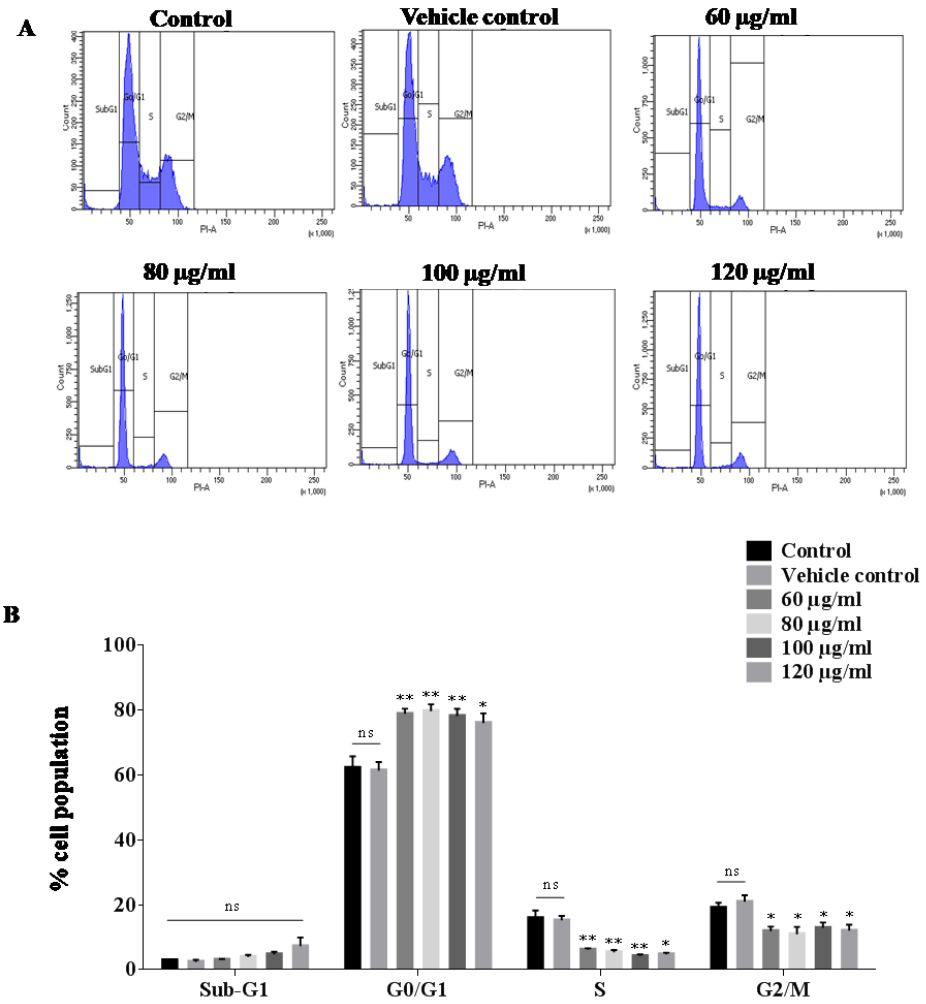

Figure 2. **LCLE induced G0/G1 cell cycle arrest in MDA-MB-231 cells. (A)** Representative images of cell cycle phase distribution of MDA-MB-231 cells following 24 hours of treatment with LCLE at different doses.**(B)** Bar diagram showing the percentage of MDA-MB-231 cells in different cell phases (G0/G1, S, G2/M, and sub-G1) of the cell cycle following 24 hours treatment of LCLE at different doses. Data are means of three independent experiments and presented as mean ± SEM where * is (P≤0.05), ** (P≤0.01), *** (P≤0.001) and **** (P≤0.0001) and ns signifies non-significant.

Figure 3

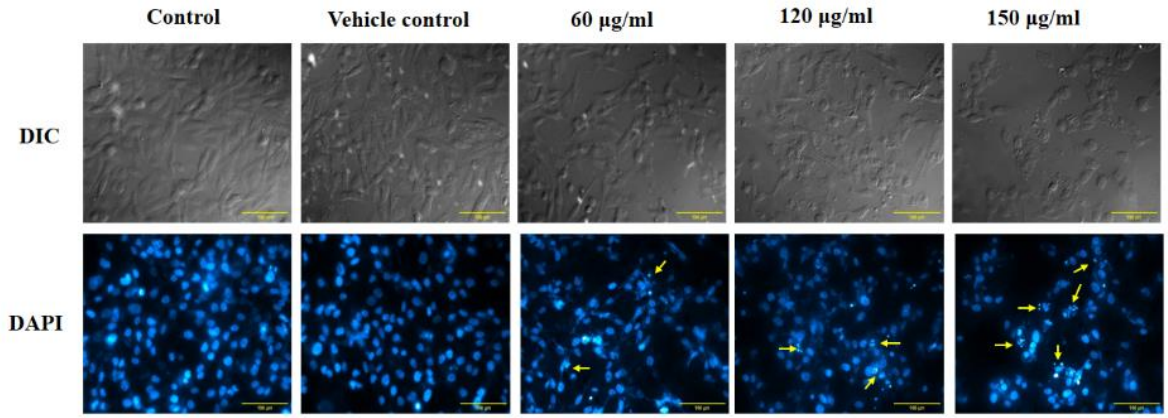

Figure 3. LCLE produced chromatin condensation. MDA-MB-231 cells were treated using different doses of LCLE for 24 hours and nuclear staining was performed using DAPI and images were taken. Condensed and fragmented nuclei are marked by arrows. Upper panel: DIC images of MDA-MB-231 for corresponding doses; Lower panel: DAPI images of MDA-MB-231 for corresponding doses.

Figure 4

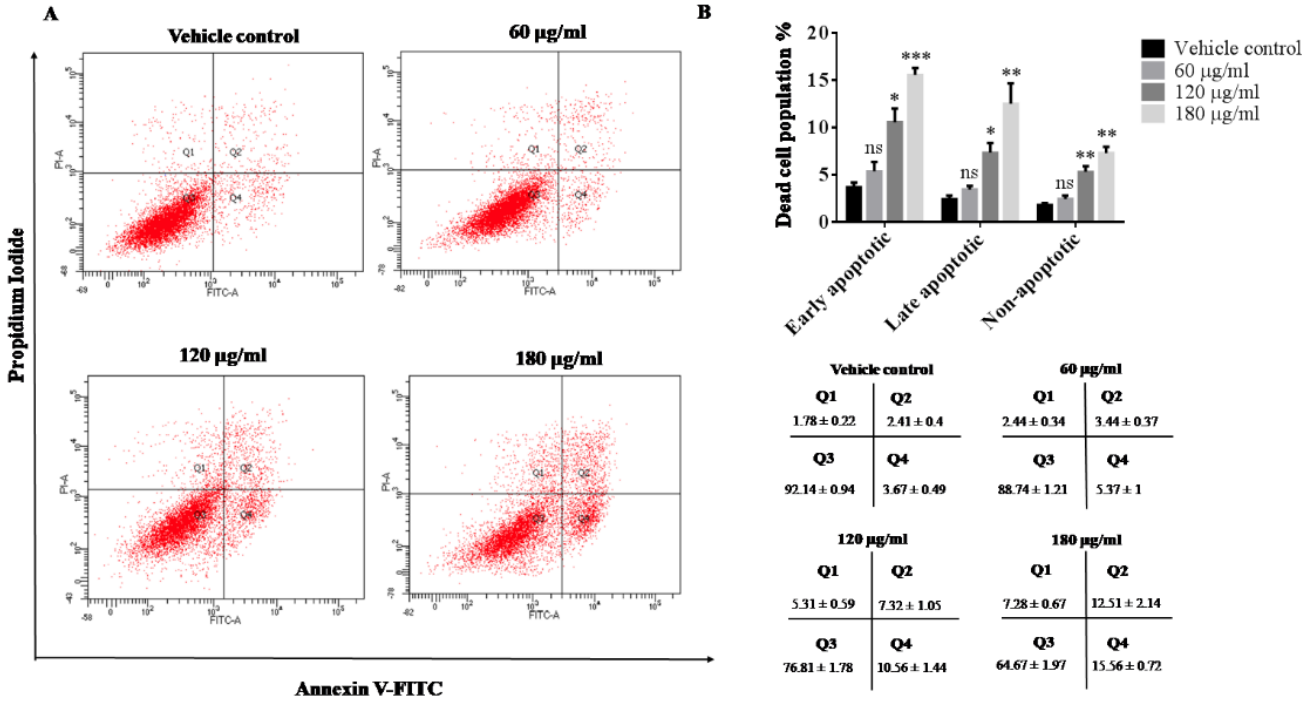

Vehicle control		60 µg/ml	
Q1	Q2	Q1	Q2
1.78 ± 0.22	2.41 ± 0.4	2.44 ± 0.34	3.44 ± 0.37
Q3	Q4	Q3	Q4
92.14 ± 0.94	3.67 ± 0.49	88.74 ± 1.21	5.37 ± 1

120 µg/ml		180 µg/ml	
Q1	Q2	Q1	Q2
5.31 ± 0.59	7.32 ± 1.05	7.28 ± 0.67	12.51 ± 2.14
Q3	Q4	Q3	Q4
76.81 ± 1.78	10.56 ± 1.44	64.67 ± 1.97	15.56 ± 0.72

Figure 4. LCLE promoted apoptosis in MDA-MB-231 cells. MDA-MB-231 cells were treated using different doses of LCLE for 24 hours followed by double staining the cells with Annexin V-FITC/PI and further analyzed using flow cytometer. **(A)** Scatter analysis with Annexin V-FITC/PI double staining represents the percentage of viable MDA-MB-231 cells (lower left quadrant, Q3) and cells undergoing early apoptosis (lower right quadrant, Q4), late apoptosis (upper right quadrant, Q2) and non-apoptotic (upper left quadrant, Q1) mode of cell death upon treatment with various doses of LCLE for 24 hours **(B)** Upper panel: Bar diagram represents the percentage of non-viable cell population in early apoptotic, late apoptotic and non-apoptotic phases . Data is represented as mean ± SEM of three independent biological replicates where * is P≤0.05, ** (P≤0.01), *** (P≤0.001) and ns signifies non-significant. Lower panel: Data represents mean ± SEM. of percentage of cells distributed in Q1, Q2, Q3 and Q4.

Figure 5

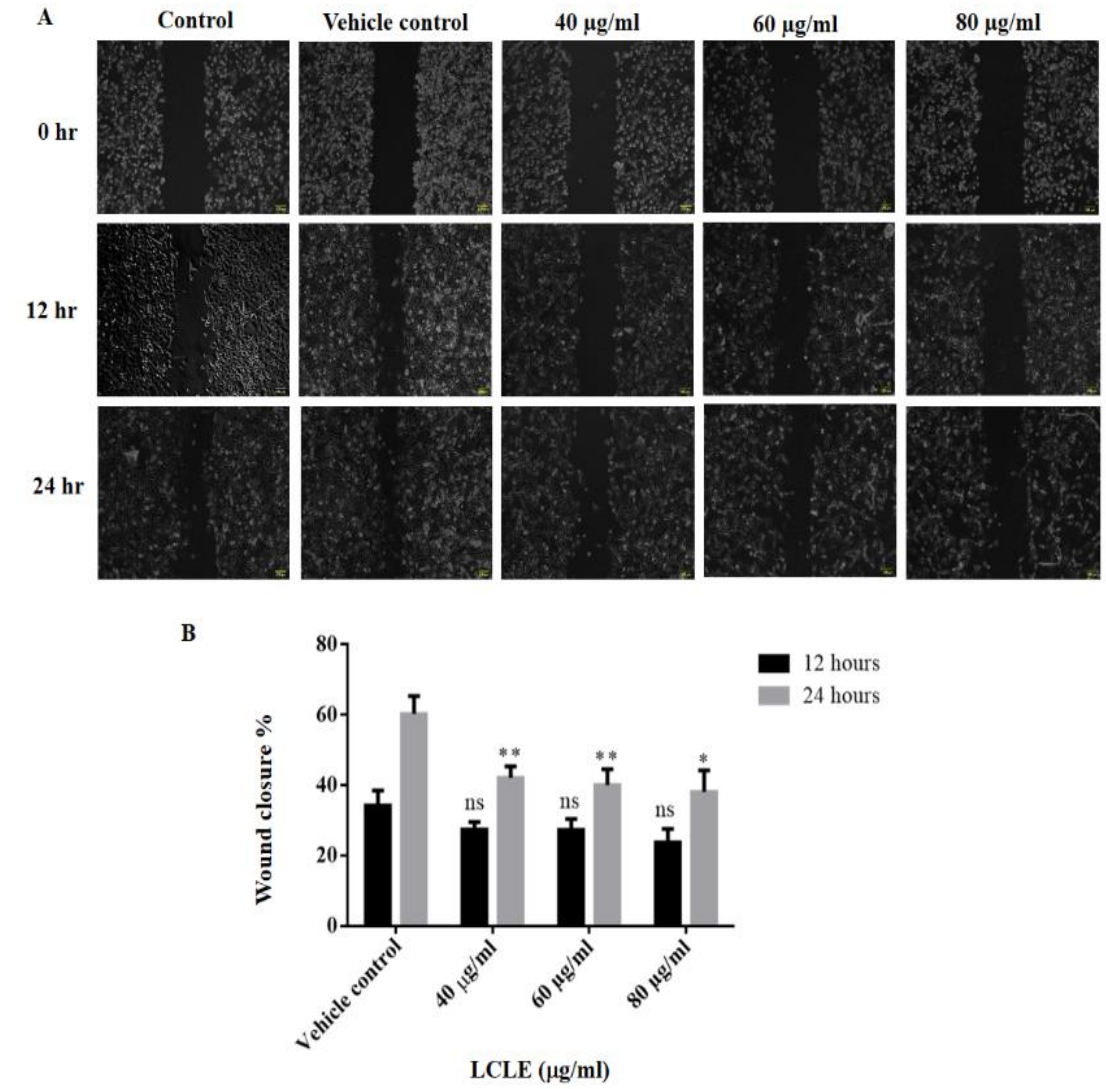

Figure 5. Migration of MDA-MB-231 cells was impeded by LCLE. (A) For wound healing assay untreated, vehicle treated and extract treated MDA-MB-231 cells were subjected to scratch at monolayer condition and then incubated for another 24 hours. Wound closure was visualized with a phase contrast microscope and images were captured at specified time intervals. **(B)** Bar diagram representing wound closure potential of MDA-MB-231 cells at different time intervals after being treated with various doses of LCLE. Data is represented as means ± SEM of three independent biological replicates where * is P≤0.05, ** (P≤0.01), *** (P≤0.001) and ns signifies non-significant.